International Journal of Biological Macromolecules 113 (2018) 1032–1040

Contents lists available at ScienceDirect

International Journal of Biological Macromolecules

journal homepage: http://www.elsevier.com/locate/ijbiomac

Thimerosal changes protein conformation and increase the rate of fibrillation in physiological conditions: Spectroscopic studies using bovine serum albumin (BSA)

João César N. Santos [a], Isabella M. da Silva [a], Taniris C. Braga [b], Ângelo de Fátima [b], Isis M. Figueiredo [a], Josué Carinhanha Caldas Santos [a,*,1]

[a] Laboratório de Instrumentação e Desenvolvimento em Química Analítica (LINQA), Instituto de Química e Biotecnologia, Universidade Federal de Alagoas, Maceió, AL 57072-900, Brazil
[b] Grupo de Estudos em Química Orgânica e Biológica (GEQOB), Departamento de Química, Universidade Federal de Minas Gerais, Belo Horizonte, MG 31270-901, Brazil

ARTICLE INFO

Article history:
Received 11 January 2018
Received in revised form 11 February 2018
Accepted 18 February 2018
Available online 21 February 2018

Keywords:
Thimerosal
BSA and ethylmercury
Interaction mechanism
Protein fibrillation

ABSTRACT

The interaction between bovine serum albumin (BSA) and thimerosal (TM), an organomercury compound widely employed as a preservative in vaccines, was investigated simulating physiological conditions and using different spectroscopic techniques. The results, employing molecular fluorescence showed the interaction occurs by static quenching through electrostatic forces ($\Delta H < 0$ and $\Delta S > 0$), spontaneously ($\Delta G = -4.40$ kJ mol^{-1}) and with a binding constant of 3.24×10^3 M^{-1}. Three-dimensional fluorescence studies indicated that TM causes structural changes in the polypeptide chain of the BSA, confirmed by circular dichroism that showed an increase in α-helix (from 43.9 to 47.8%) content after interaction process. Through synchronized fluorescence and employing bilirubin as a protein site marker, it was confirmed the preferential interaction of TM in the subdomain IB of BSA. The interaction mechanism proposed in this work is based on the reaction of TM with BSA through of free Cys34 residue, forming the adduct BSA-HgEt with the thiosalicylic acid release, which possibly interacts electrostatically with positive side chain amino acids of the modified protein. Finally, it was proven that both TM and EtHgCl accelerate the protein fibrillation kinetics in 42 and 122%, respectively, indicating the toxicity of these compounds in biological systems.

1. Introduction

Thimerosal (TM, Fig. 1) is an organomercury compound containing 49.55% of mercury mass and may form ethylmercury in the aqueous medium. TM is used as a preservative in pharmaceutical products, cosmetics, antiseptic spray, cleaning products and vaccines because it has bactericidal and antifungal properties [1]. Hepatitis B, H1N1, and triple viral vaccines are some examples of the use of this preservative, where the declared TM concentration is of the order of 25 μg Hg per 0.5 mL [2]. Regarding this aspect, several studies show a relation of the use of TM associated with deleterious effects on health, mainly in children and pregnant women.

Goldman [3] demonstrated the application of a single dose of vaccine containing TM in pregnant women within the first eight weeks of gestation could generate a fetal exposure to mercury about 125,000 times the Environmental Protection Agency (US EPA) allowable value, resulting in the inadequate formation and even fetal death [3]. According to Geier et al. [4], children that receive doses of TM from vaccines in the first months of life are more prone to develop neurological disorders such as autism and hyperactivity. Lee et al. [5] showed TM induces to oxidative stress in epithelial cells leading them to apoptosis, indicating the cytotoxicity of this compound [5]. Harmful effects of TM are under constant investigation due to this compound is the third largest way of mercury contamination, being supplanted by the exposure through dental amalgams that has in its composition elemental mercury and by the ingestion of foods contaminated with methylmercury such as fish and rice [6].

In general, organic compounds of mercury are more toxic than inorganic. For example, the IC_{50} for neural cells is 1.15 to 10.31 μM for the methylmercury and 6.44 to 160.97 μM for the Hg(II) [7]. In this context, the damage associated with TM is mainly due to the cleavage of the S—Hg bound with the possible release of ethylmercury, a neurotoxin, which presents toxicity compared to the methylmercury [8]. Despite the evidence of toxicity to human health and environmental contamination [6], the United States and other countries still use the TM neglecting its potentially harmful effects [9].

Thimerosal in biological medium can interact with biomolecules and be distributed through several tissues. One of these (bio)macromolecules

* Corresponding author.
E-mail address: josue@iqb.ufal.br (J.C.C. Santos).
[1] This work is dedicated to Prof. Mauro Korn (Universidade do Estado da Bahia - UNEB, Bahia, Brazil) for his ability to inspire their students.

https://doi.org/10.1016/j.ijbiomac.2018.02.116
0141-8130/

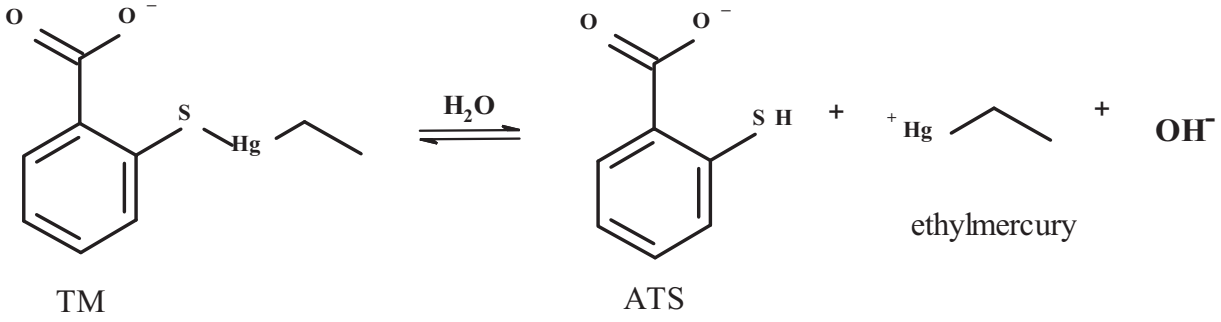

Fig. 1. Thimerosal (TM) equilibrium in aqueous medium forming the thiosalicylic acid (TSA) and ethylmercury ($EtHg^+$).

is the albumin, the most abundant protein in plasma in the human body and its main function is the transport of fatty acids, metal ions, drugs, vitamins, hormones, among other species [10]. The protein BSA (bovine serum albumin) is employed as a model for the HSA (human serum albumin) due to the similarity of 76% in the amino acid sequence and homology of 80% [11]. This protein contains three domains structurally similar classified as I, II and III, which are subdivided in subdomain A and B [12]. In its structure there are two regions where the probability of interaction is greater, called sites I and II located in the subdomains IIA and IIIA, respectively [13]. The main differences between these albumins are the tryptophan residues number. The HSA has only one (Trp214), while the BSA has two residues, one at the site I (Trp213) and the other near the subdomain IB (Trp134), where there is the only free cysteine residue (Cys34), in both proteins [14].

Some studies demonstrated the formation of adducts between Hg(II), $MeHg^+$, $EtHg^+$, phenylmercury, among other species, with HSA and BSA from the bound with thiol groups present in biomolecules [15]. Trümpler et al. simulating conditions of an intravenous injection showed the presence of proteins accelerates the TM hydrolysis process, resulting in the formation of $EtHg^+$, which reacts with the free cysteine residue of protein [16]. In addition, Guo et al. [17] demonstrated organomercurials specificity for regions containing sulfhydryl groups in peptides and proteins. Chunmei et al. [19] and Shen et al. [18] evaluated the interaction between Hg(II) and BSA and verified changes in the secondary structure of the protein. The variations in the protein structure induced by mercury and derivatives may represent a defense mechanism, since when albumin binding to toxic species of mercury prevents them from remaining in free form in the biological environment. In contrast, it may also be associated with a more efficient distribution of these species in the body, affecting different physiological functions [20].

There are few studies about the interaction between species derived from mercury with carrier proteins to explain the possible loss or not of its functionality. However, these works not mention the preferential region where the interaction occurs in the protein, the interaction mechanism is not proposed, and the experiments are performed under non-physiological conditions [15,19,20]. Therefore, is pertinent to evaluate the interaction between carrier proteins and TM aiming to clarify the main parameters associated with the interaction process, to contribute to the understanding of the possible damages caused by the TM to the organism.

In this work, we evaluated the interaction between BSA and TM simulating physiological conditions using spectroscopic techniques such as molecular fluorescence, UV–vis, circular dichroism (CD) and nuclear magnetic resonance (NMR). Thus, the magnitude of the interaction, thermodynamic parameters, forces that act on this process, preferential binding site and the structural changes in the protein were verified. Finally, we propose the mechanism of interaction and suggest one of the possible causes of TM toxicity may be associated with its ability to induce the protein fibrillation, which is related to several conformational diseases.

2. Experimental

2.1. Reagents and solutions

Bovine serum albumin (BSA, purity ≥ 98%), thimerosal (purity 97–101%), warfarin, ibuprofen, diazepam, bilirubin, 5,5′-dithiobis-2-nitrobenzoic acid (DTNB), EtHgCl, *N*-ethylmaleimide (NEM), thiosalicylic acid (TSA), 2,2′-dithiodibenzoic acid (DTSA), cysteine and thioflavin T were obtained from Sigma-Aldrich (USA). Other reagents employed in the assays were of analytical grade with purity above 98%. Stock and work solutions of TM (1 mM) and BSA (100 μM) were prepared in 50 mM Tris-HCl buffer (pH 7.4 ± 0.1) with NaCl 100 mM for ionic strength adjustment. Ultrapure water (18.2 MΩ cm^{-1}) was used in all the experiments to prepare the solutions (Millipore, USA). The differences in the concentrations of BSA and TM used are related to the sensitivity and specificities of each technique or method employed.

2.2. Molecular fluorescence

The steady-state molecular fluorescence spectra were obtained using a spectrofluorophotometer model RF-5301PC (Shimadzu, Japan) with a xenon lamp (150 W) as radiation source. The measurements were made in a quartz cuvette with an optical path of 10 mm. The slit used in all experiments was 5 nm for excitation and emission, respectively. In the spectrofluorometric titrations of protein ($\lambda_{ex}/\lambda_{em}$ = 280/342 nm), increasing increments of TM (0–80 μM) was added in BSA solution (2 μM) at different temperatures (22, 30 and 38 °C). In this procedure, λ_{ex} = 280 nm was employed to obtain overall information on the interaction process considering the Tyr and Trp residues.

The ionic strength influence was evaluated from the variation of the NaCl concentration (0–150 mM). For the 3D-fluorescence experiments, BSA solutions (2 μM) in the absence and presence of TM (50 μM) were excited in the 220–340 nm range with emission spectra recorded from 270 to 450 nm. Synchronous fluorescence studies were applied to monitor the tryptophan (Δλ = 60 nm) and tyrosine (Δλ = 15 nm) residues separately, as well as the evaluation of the polarity of the microenvironment of these amino acids [19]. For the evaluation of the binding sites in the BSA were used warfarin (site I), ibuprofen and diazepam (site II) [21,22]. The subdomain IB was monitored using bilirubin [23]. The effect of competitors present in the plasma under physiological conditions was evaluated considering physiological normality concentration. All experiments exploring molecular fluorescence were performed at 30 °C, except the spectrofluorometric titration, which was carried out at three different temperatures.

2.3. Molecular absorption spectrometry (UV–vis)

The UV–vis measurements were performed using spectrophotometer AJX-6100PC (Micronal, Brazil) of double beam equipped with a quartz cuvettes pair having 10 mm of optical path. The spectra of solutions of BSA

(3 μM), TM (12 μM) and the respective mixture (BSA + TM) were obtained in the absorbance module at 30 °C.

2.4. Circular dichroism (CD)

CD measurements were recorded on a Jasco spectropolarimeter (model J-815, Japan) and Peltier type cooling system. A quartz cuvette of 0.1 mm optical path was used, being each spectrum the average of four scans at 50 nm min^{-1}. The measurements were performed in the 200–260 nm range with 1.0 nm bandwidth and BSA (2 μM) was titrated with TM (0, 2, 4 and 8 μM) at 22 °C [15,19].

2.5. Ellman's assay

For the spectrophotometric quantification of the free thiol group (Cys34) present in the BSA it was applied the Ellman's assay. This test is based on the reaction between DTNB (1 mM) and the thiol group leading to the formation of the chromophore (TNB) in phosphate buffer (pH 7.4) with $\lambda_{max} = 412$ nm [24]. The cysteine was used as a reference and NEM as the control compound for blocking the thiol group in the BSA. The influence of EtHgCl, TSA and TM on the total free thiol group content in the BSA was evaluated at 30 °C. The concentration of all compounds was fixed at 60 μM.

2.6. Nuclear magnetic resonance (NMR)

The interaction between BSA and TM by ^{1}H NMR were evaluated by TM (1 mM) spectra profile in the absence and presence of 10, 20 and 40 μM BSA. Experiments were performed with salicylic acid (1 mM), EtHgCl (1 mM), cysteine (1 mM) and the mixtures TSA + EtHgCl and TM + Cys. The spectra were obtained on a Bruker 400 MHz spectrometer ($B_0 = 9.4$ T), using an indirect detection probe of 5 nm at 22 °C. The solutions were prepared in 10 mM phosphate buffer (pH 7.4) using H_2O/D_2O (1:10) containing 40 μM sodium trimethylsilylpropionate (TMSP). In the experiments containing the mixture TM and BSA the resolution, peaks multiplicity, and variation of the chemical shift (δ) were used as evaluation parameter.

2.7. Evaluation of amyloid formation

In the fibrillation assay, was used BSA solution (2.5 mg L^{-1}) in the absence and presence of TM and EtHgCl (both at 100 μM) and thioflavin T (ThT, 20 μM) as fluorescent probe to detect the amyloid formation. The solutions were maintained at 70 °C until 7 h, and aliquots of 10 μL were removed from the system at defined time intervals, added to 990 μL of the ThT solution and the emission signal was recorded ($\lambda_{ex}/\lambda_{em} = 442/488$ nm) at 30 °C [25].

3. Results and discussion

3.1. Binding and thermodynamic parameters

The residues of tryptophan (Trp) and tyrosine (Tyr) are the main responsible for the fluorescence emission in proteins and are used to monitor conformational changes resulting from the interaction between the fluorophore (protein) and the quencher (ligand) [26–28]. To evaluate the BSA interaction under simulated physiological conditions the protein was titrated with TM, being the variation of the fluorescence signal of the macromolecule monitored at 342 nm. Fig. 2a shows the addition of increasing concentrations of TM there was suppression of fluorescence of BSA without a shift in the protein emission wavelength and the TM does not shows intrinsic fluorescence. This result demonstrates the occurrence of interaction between the macromolecule and ligand with the formation of a non-fluorescent complex between BSA-TM.

Mathematical treatments were carried out to evaluate the interaction of the complex formed between BSA-TM. The constant of Stern-Volmer (K_{SV}) indicates the efficiency of the quencher (ligand) in suppressing the fluorescence of the fluorophore (BSA) [29]:

$$\frac{F_0}{F} = 1 + K_{SV}[Q] \quad (1)$$

F_0 and F are the fluorescence signals in the absence and presence of the ligand, respectively. [Q] is the concentration of quencher (TM) and K_{SV} is the Stern-Volmer constant. K_{SV} is obtained from the slope of linear relation F_0/F *vs* [Q] (Fig. 2b).

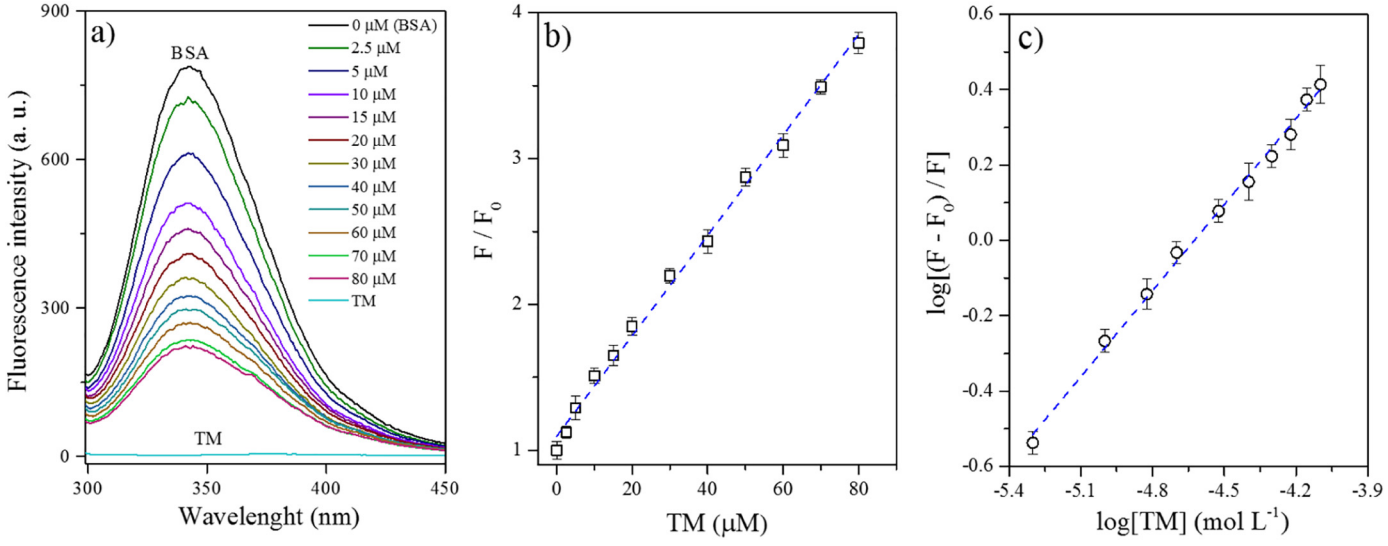

Fig. 2. a) Emission spectral profile of BSA (2 μM) at increasing concentration of TM (0–80 μM). b) Stern-Volmer quenching plot. c) Double logarithmic curve for calculation of the binding constant. Conditions: pH of 7.4 at 30 °C. Experiments performed in triplicate.

The calculation of the binding constant (K_b) reveals the strength of the interaction between the protein and the ligand, as well as the number of binding sites (n) between BSA and TM [30]:

$$\log\left[\frac{F_0 - F}{F}\right] = K_b + n \log[Q] \quad (2)$$

K_b is the binding constant obtained from the determination of the intercept of the equation (Fig. 2c), and n is the number of binding sites (stoichiometry) between BSA and TM.

The reduction in the protein fluorescence signal with the addition of TM indicates that there was energy transferring from the macromolecule to the quencher [31]. The K_{SV} values were calculated for three temperatures (22, 30 and 38 °C) ranging from 2.96 to $3.09 \times 10^4\ M^{-1}$ (Table 1), which shows quantitatively the interaction between BSA and TM.

The dominant quenching mechanism in the protein-ligand interaction process could be established for the evaluation of the K_{SV} variation in function of the temperature. In the interaction process, may occur two types of preferential quenching, static and dynamic. The static quenching is characterized by the formation of the complex in the ground state; while in the dynamic, collisions occur between the fluorophore and the ligand, being governed by the diffusion coefficient of the compound in the medium. Table 1 shows the K_{SV} values decreasing with increases of temperature, indicating prevalence of the static quenching mechanism [26,27].

The K_b values for the BSA-TM interaction ranged from 2.95 to $4.13 \times 10^3\ M^{-1}$ based on temperature variation (Table 1) and the n was close to unity indicating molar proportion of 1:1 between TM and BSA. The K_b values obtained for the TM were higher when compared to the studies between BSA and Hg(II) performed by Chunmei et al. [19] ($K_b = 0.9 \times 10^3\ M^{-1}$) and Shen et al. [18] ($K_b = 0.27 \times 10^3\ M^{-1}$). These values were indicating higher affinity of the protein for the TM.

The thermodynamic parameters were calculated based on the variation of the K_b in function of the temperature. From the Van't Hoff equation [32] the values of ΔH and ΔS were determined:

$$\ln K_b = -\frac{\Delta H}{R}\left[\frac{1}{T}\right] + \frac{\Delta S}{R} \quad (3)$$

T is the temperature in Kelvin (K), and R is the universal gas constant. These parameters were calculated from the slope and intercept of relation $\ln K_b$ *vs* 1/T (Fig. S1). The ΔG value was obtained using the following equation:

$$\Delta G = \Delta H - T\Delta S \quad (4)$$

The calculated thermodynamic parameters are presented in Table 1. According to Ross and Subramanian [33], if $\Delta H < 0$ ($-16.10\ kJ\ mol^{-1}$) and $\Delta S > 0$ ($+14.46\ J\ mol^{-1}\ K^{-1}$) the interaction between BSA-TM is governed by electrostatic forces. Additionally, all values of ΔG were negative indicating the spontaneity of the interaction.

This result is in agreement with the negative charge present in the TM (Fig. 1). The pK_a of the TM is 3.05 [34] and under physiological conditions (pH 7.4) will be completely dissociated, possibility electrostatic interaction through the positive amino acid residues of BSA. The evaluation of ionic strength influence confirmed the electrostatic interactions in the BSA-TM system (Supplementary content).

3.1.1. Competitors evaluation in the BSA-TM interaction process

In the plasma, several species can bind to albumin and, thus, favor or hinder the transport of substances in the biological environment. Therefore, was evaluated the influence of 15 possible competitors considering physiological normality concentration (Table S1) in the BSA-TM interaction process. The influence of these competitors could be assessed by the variation of the binding constant in the absence (K_b) and presence (K_b') of these species. Thus, the ratio between the constants of the interaction BSA-TM in the presence and absence of the competitor (K_b'/K_b) was the parameter used for this evaluation. If $K_b'/K_b > 1$ indicates that the evaluated species favors the interaction process between BSA and TM, the opposite $K_b'/K_b < 1$, is related to the disadvantage of the interaction. Most of the competitors did not significantly influence the interaction process simulating the physiological conditions, since the constant ratio was close to unity (Fig. S3). However, Ca(II) and Fe(II) did not follow this trend. There is a strong affinity between TM and Ca (II) in intracellular systems [35] which may be related to increase of the K_b. Moreover, Ca(II) and Fe(II) may be acting allosterically, causing structural changes in the biomolecule and contributing for interaction with TM [36].

3.2. UV–vis evaluation of interaction process

The UV–vis spectroscopy was employed to confirm the formation of the BSA-TM complex by monitoring structural changes of the protein as well as establishing the quenching mechanism associated with the fluorescence suppression process [37].

The free BSA showed maximum absorption at 278 nm (Fig. S4) and the aromatic residues of tryptophan, tyrosine and phenylalanine are the main amino acids responsible for this absorption due to the transitions $\pi \rightarrow \pi^*$ [38]. When TM was added to the BSA solution, occurred a hyperchromic effect followed by a 5 nm hypochromic shift, indicating an interaction between BSA and TM and the formation of the supramolecular complex (BSA-TM). This affirmation was based on the resulting spectrum from the subtraction of the system BSA-TM spectra by the free ligand (TM) generated in a non-overlapping spectrum to the free BSA spectrum (Fig. S4). Additionally, it was found that complex absorbance value at a maximal wavelength ($A_{BSA\text{-}TM} = 0.152$) was different from the sum of the free TM and free BSA absorbance values ($A_{TM} + A_{BSA} = 0.034 + 0.108 = 0.142$). This result evidence there was no additive effect of Beer's law ($A_{TM} + A_{BSA} \neq A_{BSA\text{-}TM}$) and confirming the protein and TM complex formation [39].

Finally, the BSA-TM complex formation demonstrated by UV–vis is associated with changes in the ground state of the involved species in the interaction process [40], confirming the static quenching mechanism previously reported by molecular fluorescence results.

3.3. Evaluation of conformational changes in the structure of BSA

3.3.1. 3D fluorescence

Conformational variations in the protein structure when interacting with the TM can be evaluated by 3D fluorescence, through characteristic changes of the emission bands related to the polypeptide chain and the

Table 1
Binding and thermodynamic parameters for the interaction between BSA and TM at different temperatures. Experiments performed in triplicate.

T (°C)	Binding parameters					Thermodynamic parameters		
	K_{SV} ($10^4\ M^{-1}$)	r	K_b ($10^3\ M^{-1}$)	r	n	ΔH ($kJ\ mol^{-1}$)	ΔS ($J\ mol^{-1}\ K^{-1}$)	ΔG ($kJ\ mol^{-1}$)
22 (295 K)	3.09 ± 0.03	0.9987	4.13 ± 0.03	0.9974	1.03 ± 0.04			−4.28
30 (303 K)	3.01 ± 0.04	0.9978	3.24 ± 0.01	0.9971	1.01 ± 0.02	−16.10	+14.46	−4.40
38 (311 K)	2.96 ± 0.02	0.9969	2.95 ± 0.02	0.9963	1.00 ± 0.03			−4.51

r = linear correlation coefficient.

tryptophan and tyrosine residues [41]. Fig. 3a shows the 3D fluorescence spectrum for the BSA, where three peaks stand out. The first one refers to the Rayleigh scattering, in which the wavelength of excitation is equal to the emission ($\lambda_{ex} = \lambda_{em}$), associated with the inelastic radiation scattering. The residues of tryptophan and tyrosine are responsible for the emission band correspondent to peak 2 ($\lambda_{ex}/\lambda_{em} = 285/342$ nm). Peak 3 is related to the polypeptide chain ($\lambda_{ex}/\lambda_{em} = 238/335$ nm) showing transition $\pi \rightarrow \pi^*$ due to the group C═O (in the peptide bond) typical of the secondary structure of the protein [41,42]. According to Fig. 3b peaks 2 and 3 in the 3D fluorescence emission spectrum of the BSA-TM system reduced the emission intensity in 50.4 and 59.2%, respectively, due to the interaction process (Table S2). In addition, the Stokes shift of peaks 2 and 3 was altered when TM was added indicating changes in polarity/conformation of native protein may have occurred [43], which may lead to damage or functional changes.

3.3.2. Circular dichroism (CD)

Alterations in the protein secondary structure can be detected by the CD technique. The content of α-helix present in the protein exhibits negative bands at 208 and 222 nm, due to the $\pi \rightarrow \pi^*$ and $n \rightarrow \pi^*$ transitions of the polypeptide chain [44–46]. The values expressed by CD are given regarding the mean residue elliptic (MRE), according to [47]:

$$\text{MRE} = \frac{\text{observed CD(m med)}}{C_p \times n \times L \times 10} \left(\text{deg cm}^2\ \text{dmol}^{-1} \right) \quad (5)$$

C_p is the molar concentration of the protein (2 μM), n is the number of amino acid residues (583 for BSA), and L is the length of the optical path (0.1 cm). The amount of α-helix was calculated using the equation:

$$\alpha\text{-helix}(\%) = \frac{(-\text{MRE}_{208} - 4000)}{(33000 - 4000)} \times 100 \quad (6)$$

MRE_{208} represent the MRE values at 208, 4000 is the MRE of the β-form and random coil conformation cross and 33,000 is the MRE value of pure α-helix at 208 nm [47].

Fig. 3c shows CD spectrum profile of the BSA in function of the TM concentration variation. The protein showed, in both bands, 208 and 222 nm, increasing of intensity with the addition of the ligand to the system. In the absence of TM, the calculated α-helix content was 43.9%, when increases the TM ratio (1:1, 1:2 and 1:4) the α-helix content increased for both bands, in 45.1, 46.0 and 47.8%, respectively, and no shift in the minima absorption wavelength was observed.

The increase in the α-helix content of the evaluated system can be associated with the electrostatic interaction of the negative charge in the TM with the positive charges present on the surface of the BSA. This situation provides a more stable structure of the protein, with increased content of α-helix due to inter or intramolecular dipole-dipole interactions [48]. In this way, the binding of TM to BSA causes changes in the secondary structure of the protein. A similar profile was observed by Chunmei et al. [19] in the evaluation of the interaction between BSA (2 μM) and Hg(II) (0–20 μM) with the increasing of α-helix content from 50.93 to 56.29%. Moreover, Li et al. [15], evaluate the interaction between HSA with Hg(II) and other species of mercury ($MeHg^+$, $EtHg^+$ and $PhHg^+$), also found changes in the secondary structure of the protein after incubation for 12 h in the 1:10 ratio (HSA-ligand at 1.5 and 15 μM, respectively). However, an increase in the content of β-sheet from 4.7 to 10% was observed after the interaction.

3.4. Synchronous fluorescence

Through the synchronous fluorescence, it is possible to monitor the interaction process with the tryptophan and tyrosine residues, separately (Fig. S5a). For this, it remains constant $\Delta\lambda$ in function of the λ_{ex}, being $\Delta\lambda = 60$ nm to monitor the residues of Trp selectively, and in an analogous way when using $\Delta\lambda = 15$ nm, the Tyr residue is observed. In addition, this assay can identify polarity changes in the microenvironment of these amino acid residues as a function of the interaction process [49,50].

Fig. S5b and c shows the synchronized fluorescence spectra profiles of the Tyr and Trp residues with maxima emission at 299 and 337 nm, respectively. After addition of TM, the fluorescence intensity of the BSA decreased without a change in the maximum emission of Tyr (Fig. S5b). However, a red shift of 2 nm was observed for the Trp followed by reduction of the fluorescence signal when interacts with TM (Fig. S5c), indicating that the microenvironment near this amino acid becomes more polar and accessible to the solvent (water) [51]. Moreover, based on Table S3, the K_{sv} value for Trp ($1.36 \pm 0.08 \times 10^4$ L mol^{-1}) is higher compared to Tyr ($0.46 \pm 0.03 \times 10^4$ L mol^{-1}). Thus, TM is closer to the region that contains the Trp residue in the interaction process with the protein. BSA has two residues of tryptophan, one located at site I (Trp213) and the other at subdomain IB (Trp134). Although this result indicates the proximity of the tryptophan residue in the interaction process, it cannot be inferred which one (Trp213 or Trp134) the microenvironment had more significantly altered. Chunmei et al. [19] and Shen et al. [18] obtained a similar result in the interaction study between BSA and Hg(II) by synchronous fluorescence, however, was not determined which region of the protein occurs interaction. Therefore, the preferred sites of the TM interaction in the protein structure were evaluated using specific regions markers binding of the BSA.

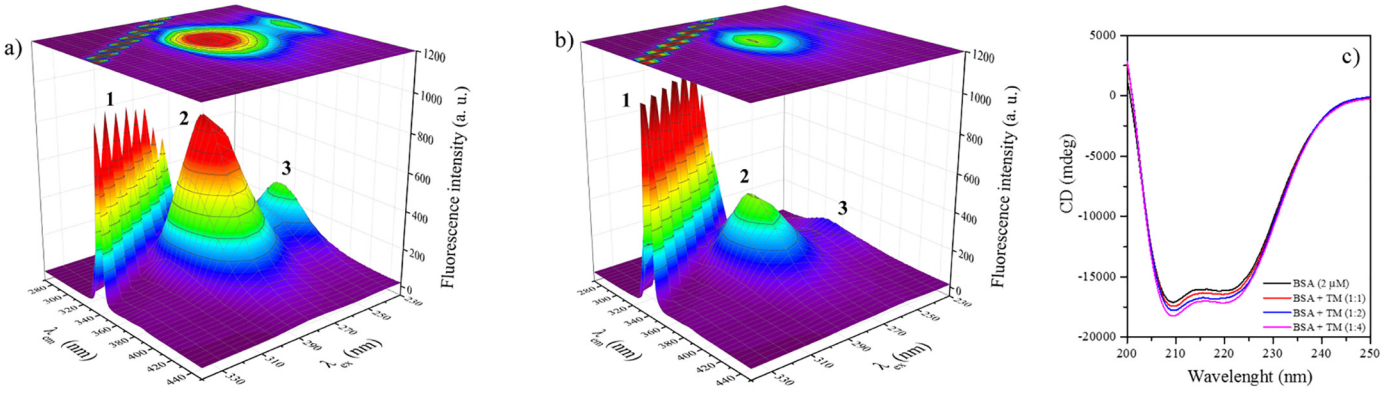

Fig. 3. Three-dimensional fluorescence spectra of a) BSA and b) BSA-TM complex at 30 °C. Protein and ligand at 2 and 50 μM, respectively. c) Circular dichroism spectra of 2 μM BSA in the presence of (2, 4 and 8 μM) TM at 22 °C.

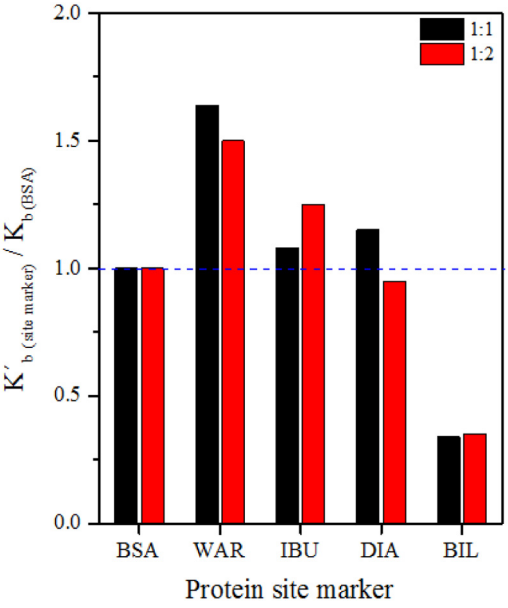

Fig. 4. The binding constant ratio for protein site markers warfarin (WAR), ibuprofen (IBU), diazepam (DIA) and bilirubin (BIL) all at 2 and 4 μM in the interaction process between BSA (2 μM) and TM (0–80 μM) at 30 °C.

3.5. Protein binding site

In the BSA there are two preferred regions for the binding of small molecules called sites I and II. Warfarin (WAR), ibuprofen (IBU) and diazepam (DIA) (Fig. S6) are preferred markers for these regions, in which warfarin binds to site I while ibuprofen and diazepam to site II [29,52]. Therefore, assays in the presence of these site markers promote competition for these protein-binding regions. A reduction in the K_b value of BSA and ligand in the presence of the site marker is an indication that both interact with the same protein region. Thus, it was considered the ratio of the constants in the presence (K_b') and in the absence (K_b) of this protein site marker as a parameter to identify the preferential binding site of TM to BSA. If this ratio is less than the unity, indicates competition for the same protein-binding site with the marker. All experiments were performed with two distinct ratios of BSA and site markers (1:1 and 1:2). Fig. 4 shows no decrease in binding constant (K_b), indicating that TM does not migrate to site I and II of the BSA.

In the previous analysis exploring synchronous fluorescence the microenvironment of the Trp residues were more influenced in the in the interaction process with TM than Tyr residues. Considering that the BSA has two Trp residues, one at the site I (Trp213) and another at subdomain IB (Trp134), and the site I residue was not altered, since TM did not displace the warfarin (site I). Thus, the Trp134 residue in subdomain IB was the main responsible for the changes observed in the synchronous fluorescence.

In the subdomain IB of BSA is present the only residue of free cysteine (Cys34) and, knowing the high affinity of mercury compounds by amino acid containing sulfur [15], such as cysteine, possibly the TM would be migrating to this region and interacting with the free Cys34 residue. To confirm this hypothesis, bilirubin (BIL, Fig. S6) was used as the protein site marker for the subdomain IB [53]. Zunszain et al. [54] found the bilirubin (BIL) binds selectively to the subdomain IB through crystallography studies. Thus, when bilirubin was added to the system the binding constant decreases, reducing the ratio of the constants (Fig. 4). This result confirms the migration of TM to the region of the subdomain IB of the BSA, differently of traditional binding sites, I and II.

Several studies show the formation of an adduct between mercury species with thiols residues from the protein of biological importance. To corroborate this proposal Krupp et al. [55] identified the bind of methylmercury and Hg(II) to biothiols forming an adduct. Based on this, the TM may react with the free Cys34 residue in the subdomain IB of the BSA. Thus, to evaluate whether adduct formation occurs after the cleavage of the thimerosal S—Hg binding in the presence of the protein, the reaction/interaction mechanism of TM with the BSA was investigated.

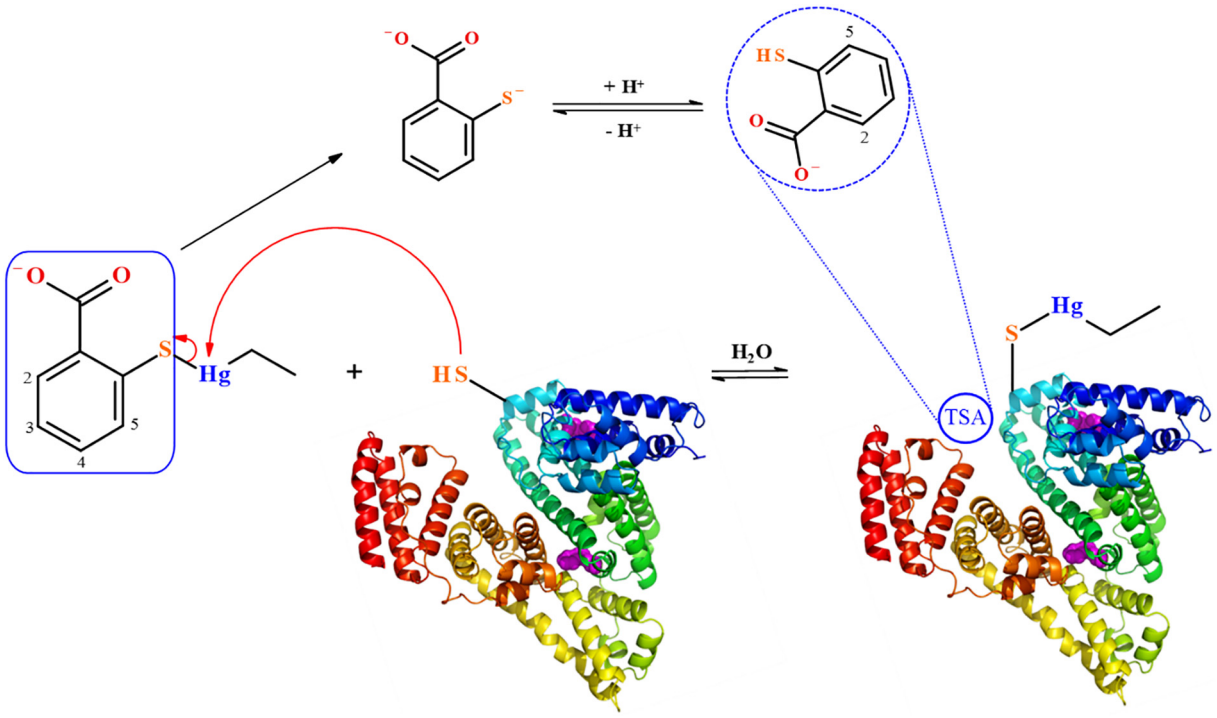

Fig. 5. Generic mechanism of reaction/interaction proposed for the thimerosal and BSA system under physiological conditions based on experimental evidences.

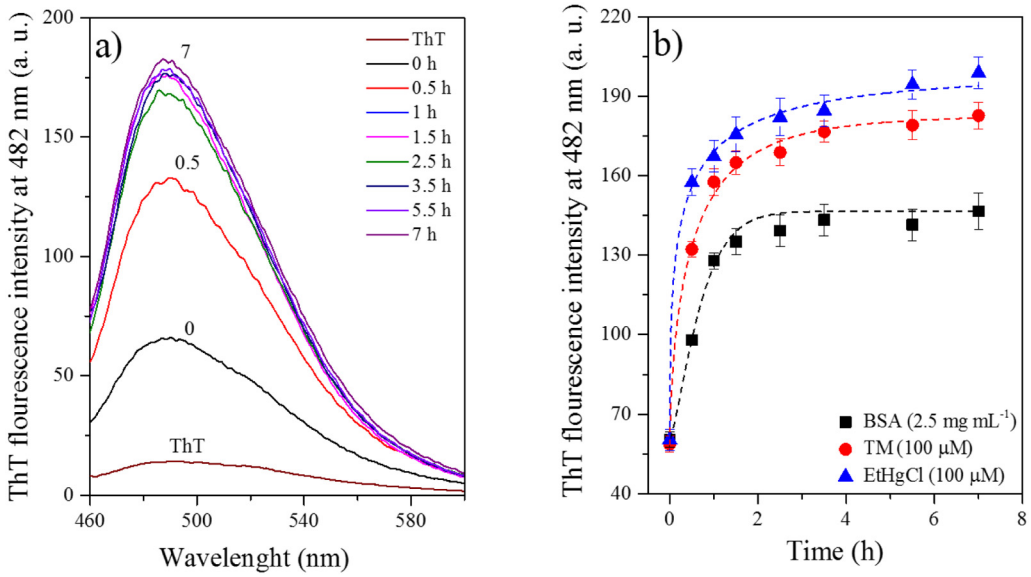

Fig. 6. a) Fluorescence spectra profile of free ThT and in the system BSA and thimerosal after incubation at 70 °C. b) Kinetics of fibrillation for free BSA in the presence of TM and EtHgCl. Experiments performed in triplicate at 30 °C.

3.6. Evaluation of interaction mechanism between TM and BSA

To propose a possible reaction/interaction mechanism between TM and BSA experiments were performed simulating physiological conditions. Therefore, was employing Ellman's assay to monitor the reactions of the free Cys34 residue, BSA interaction with TM degradation products, the monitoring of reactions involving TM and derivatives by ^{1}H NMR and application of fluorescence resonance energy transfer to determine critical distance between protein and TM (all these results are presented and discussed in Supplementary content).

Based on the different experiments the results indicate the preferential mechanism of reaction/interaction between TM and BSA must to happen in a single step. Initially, occurs the formation of an adduct BSA(Cys34)-EtHg due to cleavage S—Hg bound of TM with releasing of free TSA. Finally, the thiosalicylic acid formed will interact electrostatically in the region of the subdomain IB with positively charged amino acids (Lys131, Lys159, His49, Lys41, Lys20 and His18) of the modified protein [56]. The general mechanism of the reaction/interaction process between the TM and the BSA was generically proposed and represented in Fig. 5.

3.7. Evaluation of the amyloid formation

The formation of insoluble amyloids, rich in β-sheets with fibrillar morphology is directly related to the development of at least 25 conformational diseases such as type II diabetes, Alzheimer's and Parkinson's diseases [57–59], and some species can accelerate the fibrillation by interacting with protein, such as Cu(II), Pb(II) and carbon nanotubes [60,61].

Mercury species present high toxicity to humans and are accumulated and metabolized preferentially in the brain, where they can be biotransformed in inorganic mercury [62] and contribute directly to the process of protein fibrillation. To evaluate the effect of the possible toxicity of the TM in a biological medium, the kinetics of the protein aggregation was investigated, using EtHgCl for comparison. Thioflavin T (ThT) was used as a fluorogenic probe to monitor the amyloid formation [46]. The spectral profile obtained for the TM + BSA system about the fibrillation process is shown in Fig. 6a, indicating that free ThT has low fluorescence, but after the formation of the fibrils a significant increase of the analytical signal of fluorescence emission occurs, stabilizing after 2.5 h.

Kinetics parameters regarding the protein fibril formation (using BSA as model) were calculated in the absence and presence of TM and EtHgCl [25]:

$$F = F^{\infty} + \Delta F \exp\left(-[k_{sp}t]^{n}\right) \quad (7)$$

F is the fluorescence intensity of ThT at time t, ΔF^{∞} is the maximum fluorescence intensity, ΔF is the amplitude of the measured fluorescence emission signals, and k_{sp} is constant about the rate of spontaneous fibril formation. The effect of TM and EtHgCl for the protein fibrils induction is shown in Fig. 6b. The presence of TM and EtHgCl in the system contain BSA provides an increase in k_{sp} of 42.3 and 122.3%, respectively, when compared to the protein in the absence of the compounds (Table 2). These mercury species favored the rate of BSA fibrillation, which can promote intramolecular electrostatic repulsions favoring the formation of fibrils [62]. Additionally, the system with TM and EtHgCl presented $n < 1$ indicating the kinetics fibrillation may be associated with multiple mechanisms of the amyloid formation. Finally, the contribution of TM and EtHgCl in the process of protein fibrillation, suggest its toxic effects may be related to conformational diseases or biochemical processes associated with protein aggregation.

Table 2
Kinetics parameters of the BSA fibrillation in the absence and presence of thimerosal and EtHgCl.

System	ΔF (a. u.)	k_{sp} (h^{-1})	n
BSA (2.5 mg mL^{-1})	82	1.30 ± 0.10	1.07 ± 0.16
BSA + TM (100 µM)	124	1.85 ± 0.15	0.60 ± 0.05
BSA + EtHgCl (100 µM)	138	2.89 ± 0.43	0.40 ± 0.04

4. Conclusion

The interaction between BSA and TM simulating physiological conditions revealed static quenching with the formation of a non-fluorescent complex. The K_b value was 3.24×10^3 M^{-1} (30 °C) and the interaction process was preferably electrostatic. TM causes structural changes in the BSA structure, providing the increase in the α-helix content and, Ca(II) and Fe(II) ions favor the interaction. The thimerosal interacts preferentially in the subdomain IB of the BSA and the reaction/interaction occurs by the transfer of ethylmercury from TM to BSA,

leading to the formation of a BSA-HgEt adduct through the binding of the free Cys34 with the mercury atom. The produced TSA interacts electrostatically with positive amino acids of BSA. The distance from the TSA to the Trp134 of the BSA-HgEt adduct was 2.06 nm. Finally, the TM and EtHgCl induce the acceleration of the kinetic protein fibrillation, and this process may be one of the possible causes of the toxic action of these species in living systems.

Acknowledgements

We thank the Universidade Federal de Alagoas (UFAL), Instituto de Química e Biotecnologia (IQB), Programa de Pós-graduação em Química e Biotecnoligia (PPGQB) and the Universidade Federal de Minas Gerais (UFMG) by infrastructure, and FAPEAL (Process number 60030 000863/2016), PROCAD-CAPES (Process number: 88887.124145/2014-00), CAPES and CNPq (Process number: 306939/2015-0) for financial support and fellowships.

Appendix A. Supplementary data

Supplementary data to this article can be found online at https://doi.org/10.1016/j.ijbiomac.2018.02.116.

References

[1] D.A. Geier, P.G. King, B.S. Hooker, J.G. Dórea, J.K. Kern, L.K. Sykes, M.R. Geier, Thimerosal: clinical, epidemiologic and biochemical studies, Clin. Chim. Acta 444 (2015) 212–220.
[2] D.A. Geier, J.K. Kern, B.S. Hooker, P.G. King, L.K. Sykes, M.R. Geier, A longitudinal cohort study of the relationship between Thimerosal-containing hepatitis B vaccination and specific delays in development in the United States: assessment of attributable risk and lifetime care costs, J. Epidemiol. Global Health 6 (2016) 105–118.
[3] G. Goldman, Comparison of VAERS fetal-loss reports during three consecutive influenza seasons: was there a synergistic fetal toxicity associated with the two-vaccine 2009/2010 season? Hum. Exp. Toxicol. 32 (2013) 464–475.
[4] D.A. Geier, B.S. Hooker, J.K. Kern, P.G. King, L.K. Sykes, M.R. Geier, A two-phase study evaluating the relationship between Thimerosal-containing vaccine administration and the risk for an autism spectrum disorder diagnosis in the United States, Transl. Neurodegener. 2 (2013) 1–12.
[5] S. Lee, M.F. Mian, H. Lee, C. Kang, J. Kim, S.H. Ryu, P. Suh, E. Kim, Thimerosal induces oxidative stress in HeLa S epithelial cells, Environ. Toxicol. Pharmacol. 22 (2006) 194–199.
[6] O. Yepse, D. Contreras, P. Santander, J. Yáñez, H.D. Mansilla, D. Amarasiriwardena, Photocatalytic degradation of thimerosal in human vaccine's residues and mercury speciation of degradation by-products, Microchem. J. 121 (2015) 41–47.
[7] J. Tong, Y. Wang, Y. Lu, In vitro evaluation of inorganic and methyl mercury mediated cytotoxic effect on neural cells derived from different animal species, J. Environ. Sci. 41 (2016) 138–145.
[8] J.G. Dórea, V.L.V.A. Bezerra, V. Fajon, M. Horvat, Speciation of methyl- and ethylmercury in hair of breastfed infants acutely exposed to thimerosal-containing vaccines, Clin. Chim. Acta 412 (2011) 1563–1566.
[9] H.A. Young, D.A. Geier, M.R. Geier, Thimerosal exposure in infants and neurodevelopmental disorders: an assessment of computerized medical records in the Vaccine Safety Datalink, J. Neurol. Sci. 271 (2008) 110–118.
[10] K.A. Majoreka, P.J. Porebski, A. Dayal, M.D. Zimmermana, K. Jablonskaa, A.J. Stewart, M. Chruszcz, W. Minor, Structural and immunologic characterization of bovine, horse, and rabbit serum albumins, Mol. Immunol. 52 (2012) 174–182.
[11] E.L. Gelamo, M. Tabak, Spectroscopic studies on the interaction of bovine (BSA) and human (HSA) serum albumins with ionic surfactants, Spectrochim. Acta A 56 (2000) 2255–2271.
[12] D.C. Carter, J.X. Ho, Structure of serum albumin, Adv. Protein Chem. 45 (1994) 153–203.
[13] G. Sudlow, D.J. Birkett, D.N. Wade, The characterization of two specific drug binding sites on human serum albumin, Mol. Pharmacol. 11 (1975) 824–832.
[14] A. Sulkowska, Interaction of drugs with bovine and human serum albumin, J. Mol. Struct. 614 (2002) 227–232.
[15] Y. Li, X. Yan, C. Chen, Y. Xia, Y. Jiang, Human serum albumin-mercurial species interactions, J. Proteome Res. 6 (2007) 2277–2286.
[16] S. Trümpler, W. Lohmann, B. Meermann, W. Buscher, M. Sperling, U. Karst, Interaction of thimerosal with proteins-ethylmercury adduct formation of human serum albumin and β-lactoglobulin A, Metallomics 87 (2009) 87–91.
[17] Y. Guo, L. Chen, L. Yang, Q. Wang, Counting sulfhydryls and disulfide bonds in peptides and proteins using mercurial ions as an MS-Tag, J. Am. Soc. Mass Spectrom. 19 (2008) 1108–1113.
[18] F. Shen, Y. He, Y. Zhou, Study of interaction of mercuric chloride with bovine serum albumin by multi-spectroscopic method, Asian J. Chem. 25 (2013) 5925–5929.
[19] D. Chunmei, J. Cunwei, L. Huixiang, S. Yuze, Y. Wei, Z. Dan, Study of the interaction between mercury(II) and bovine serum albumin by spectroscopic methods, Environ. Toxicol. Pharmacol. 37 (2014) 870–877.
[20] S. Trümpler, B. Meermann, S. Nowak, W. Busher, U. Karst, M. Sperling, In vitro study of thimerosal reactions in human whole blood and plasma surrogate samples, J. Trace Elem. Med. Biol. 28 (2014) 125–130.
[21] K. Hemalatha, G. Madhumitha, Study of binding interaction between anthelmintic 2,3-dihydroquinazolin-4-ones with bovine serum albumin by spectroscopic methods, J. Lumin. 178 (2016) 163–171.
[22] Y. Ni, R. Zhub, S. Kokotc, Competitive binding of small molecules with biopolymers: a fluorescence spectroscopy and chemometrics study of the interaction of aspirin and ibuprofen with BSA, Analyst 136 (2011) 4794–4801.
[23] G.L. Ellman, K.D. Courtney, V. Andres, R.M. Featherstone, A new and rapid colorimetric determination of acetylcholinesterase activity, Biochem. Pharmacol. 7 (1961) 88–95.
[24] B. Zhao, L. Song, X. Liu, J. Xie, J. Zhao, Spectroscopic studies of the interaction between hypocrellin B and human serum albumin, Bioorg. Med. Chem. 14 (2006) 2428–2432.
[25] Y. Guan, H. Zhang, Y. Wang, New insight into the binding interaction of hydroxylated carbon nanotubes with bovine serum albumin, Spectrochim. Acta, Part A 124 (2014) 556–563.
[26] M. Siddiqi, S. Nusrat, P. Alam, S. Malik, S.K. Chaturvedi, M.R. Ajmal, A.S. Abdelhameed, R.H. Khan, Investigating the site selective binding of busulfan to human serum albumin: biophysical and molecular docking approaches, Int. J. Biol. Macromol. 107 (2018) 1414–1421.
[27] Y. Fan, S. Zhang, Q. Wang, J. Li, H. Fan, D. Shan, Interaction of an amino-functionalized ionic liquid with enzymes: a fluorescence spectroscopy study, Spectrochim. Acta A 105 (2013) 297–303.
[28] M.K. Siddiqi, P. Alam, S.K. Chaturvedi, S. Nusrat, M.R. Ajmal, A.S. Abdelhameed, R.H. Khana, Probing the interaction of cephalosporin antibiotic–ceftazidime with human serum albumin: a biophysical investigation, Int. J. Biol. Macromol. 105 (2017) 292–299.
[29] Y. Teng, R. Liu, C. Li, Q. Xia, P. Zhang, The interaction between 4-aminoantipyrine and bovine serum albumin: multiple spectroscopic and molecular docking investigations, J. Hazard. Mater. 190 (2011) 574–581.
[30] M.D.A. Dantas, H.A. Tenório, T.I.B. Lopes, H.J.V. Pereira, A.J. Marsaioli, I.M. Figueiredo, J.C.C. Santos, Interactions of tetracyclines with ovalbumin, the main allergen protein from egg white: spectroscopic and electrophoretic studies, Int. J. Biol. Macromol. 102 (2017) 505–581.
[31] X. Wu, J. Liu, Q. Wang, W. Xue, X. Yao, Y. Zhang, J. Jin, Spectroscopic and molecular modeling evidence of clozapine binding to human serum albumin at subdomain IIA, Spectrochim. Acta A 79 (2011) 1202–1209.
[32] M.M. Silva, E.O.O. Nascimento, E.F. Silva Júnior, J.X. Araújo Júnior, C.C. Santana, L.A.M. Grillo, R.S. Oliveira, P.R.R. Costa, C.D. Buarque, J.C.C. Santos, I.M. Figueiredo, Interaction between bioactive compound 11a-*N*-tosyl-5-deoxi-pterocarpan (LQB-223) and Calf thymus DNA: spectroscopic approach, electrophoresis and theoretical studies, Int. J. Biol. Macromol. 96 (2017) 223–233.
[33] P.D. Ross, S. Subramanian, Thermodynamics of protein association reactions: forces contributing to stability, Biochemistry 20 (1981) 3096–3102.
[34] H.R. Costantino, M.J. Pikal, Lyophilization of Biopharmaceuticals, first ed. AAPS, Arlington, 2005.
[35] M. Gericke, G. Droogmans, B. Nilius, Thimerosal induced changes of intracellular calcium in human endothelial cells, Cell Calcium 14 (1993) 201–207.
[36] J.P. Barnett, C.A. Blindauer, O. Kassaar, S. Khazaipoul, E.M. Martin, P.J. Sadler, A.J. Stewart, Allosteric modulation of zinc speciation by fatty acids, Biochim. Biophys. Acta 1830 (2013) 5456–5464.
[37] M.D. Meti, S.T. Nandibewoor, S.D. Joshi, U.A. More, S.A. Chimatadar, Multispectroscopic investigation of the binding interaction of fosfomycin with bovine serum albumin, J. Pharm. Anal. 5 (2015) 249–255.
[38] X. Liu, Z. Ling, X. Zhou, F. Ahmad, Y. Zhou, Comprehensive spectroscopic probing the interaction and conformation impairment of bovine serum albumin (BSA) by herbicide butachlor, J. Photochem. Photobiol. B 162 (2016) 332–339.
[39] V.D. Suryawanshi, L.S. Walekar, A.H. Gore, P.V. Anbhule, G.B. Kolekar, Spectroscopic analysis on the binding interaction of biologically active pyrimidine derivative with bovine serum albumin, J. Pharm. Anal. 6 (2016) 56–63.
[40] F. Tian, F. Jiang, X. Han, C. Xiang, Y. Ge, J. Li, Y. Zhang, R. Li, X. Ding, Y. Liu, Synthesis of a novel hydrazone derivative and biophysical studies of its interactions with bovine serum albumin by spectroscopic, electrochemical, and molecular docking methods, J. Phys. Chem. B 114 (2010) 14842–14853.
[41] Z. Cheng, R. Liu, X. Jiang, Spectroscopic studies on the interaction between tetrandrine and two serum albumins by chemometrics methods, Spectrochim. Acta A 115 (2013) 92–105.
[42] G.G. Ariga, P.N. Naik, S.T. Nandibewoor, S.A. Chimatadar, Study of fluorescence interaction and conformational changes of bovine serum albumin with histamine H_1-receptor–drug epinastine hydrochloride by spectroscopic and time-resolved fluorescence methods, Biopolymers 103 (2015) 646–657.
[43] H. Zhang, Y. Zou, E. Liu, Biophysical influence of isocarbophos on bovine serum albumin: spectroscopic probing, Spectrochim. Acta A 92 (2012) 283–288.
[44] M.K. Siddiqi, P. Alam, S.K. Chaturvedi, S. Nusrat, Y.E. Shahein, R.H. Khan, Attenuation of amyloid fibrillation in presence of Warfarin: a biophysical investigation, Int. J. Biol. Macromol. 95 (2017) 713–718.
[45] M.K. Siddiqi, P. Alam, S.K. Chaturvedi, R.H. Khan, Anti-amyloidogenic behavior and interaction of diallylsulfide with human serum albumin, Int. J. Biol. Macromol. 92 (2016) 1220–1228.
[46] P. Alam, M.K. Siddiqi, S.K. Chaturvedi, M. Zaman, R.H. Khan, Vitamin B12 offers neuronal cell protection by inhibiting Aβ-42 amyloid fibrillation, Int. J. Biol. Macromol. 99 (2017) 477–482.

[47] O.A. Chaves, B.A. Soares, M.A.M. Maciel, C.M.R. Sant'Anna, J.C. Netto-Ferreira, D. Cesarin-Sobrinho, A.B.B. Ferreira, A study of the interaction between trans-dehydrocrotonin, a bioactive natural 19-nor-clerodane, and serum albumin, J. Braz. Chem. Soc. 27 (2016) 1858–1865.
[48] A. Saha, V.V. Yakovlev, Structural changes of human serum albumin in response to a low concentration of heavy ions, J. Biophotonics 3 (2010) 670–677.
[49] T. Yuan, A.M. Weljie, H.J. Vogel, Tryptophan fluorescence quenching by methionine and selenomethionine residues of calmodulin: orientation of peptide and protein binding, Biochemistry 37 (1998) 3187–3195.
[50] R.W. Congdon, G.W. Muth, A.G. Splittgerber, The binding interaction of coomassie blue with proteins, Anal. Biochem. 213 (1993) 407–413.
[51] L. He, Z. Wang, Y. Wang, X. Liu, Y. Yanga, Y. Gao, X.W.B. Liu, X. Wang, Studies on the interaction between promethazine and human serum albumin in the presence of flavonoids by spectroscopic and molecular modeling techniques, Colloids Surf. B. Biointerfaces 145 (2016) 820–829.
[52] G. Sudlow, D.J. Birkett, D.N. Wade, Further characterization of specific drug binding sites on human serum albumin, Mol. Pharmacol. 12 (1976) 1052–1061.
[53] Ferenc Zsila, Subdomain IB is the third major drug binding region of human serum albumin: toward the three-sites model, Mol. Pharm. 10 (2013) 1668–1682.
[54] P.A. Zunszain, J. Ghuman, A.F. McDonagh, S. Curry, Crystallographic analysis of human serum albumin complexed with 4Z,15E-Bilirubin-IXα, J. Mol. Biol. 381 (2008) 394–406.
[55] E.M. Krupp, B.F. Milne, A. Mestrot, A.A. Meharg, J. Feldmann, Investigation into mercury bound to biothiols: structural identification using ESI–ion-trap MS and introduction of a method for their HPLC separation with simultaneous detection by ICP-MS and ESI-MS, Anal. Bioanal. Chem. 390 (2008) 1753–1764.
[56] P. Bolel, N. Mahapatra, S. Datta, M. Halder, Modulation of accessibility of subdomain IB in the pH-dependent interaction of bovine serum albumin with Cochineal Red A: a combined view from spectroscopy and docking simulations, J. Agric. Food Chem. 61 (2013) 4606–4613.
[57] S.K. Chaturvedi, M.K. Siddiqi, P. Alam, R.H. Khan, Protein misfolding and aggregation: mechanism, factors and detection, Process Biochem. 51 (2016) 1183–1192.
[58] M.K. Siddiqi, P. Alam, S.K. Chaturvedi, Y.E. Shahein, R.H. Khan, Mechanisms of protein aggregation and inhibition, Front. Biosci. (Elite Ed.) 9 (2017) 1–20.
[59] P. Alam, K. Siddiqi, S.K. Chturvedi, R.H. Khan, Protein aggregation: from background to inhibition strategies, Int. J. Biol. Macromol. 103 (2017) 208–2019.
[60] N.K. Pandey, S. Ghosh, S. Dasgupta, Fibrillation in human serum albumin is enhanced in the presence of copper(II), J. Phys. Chem. 114 (2010) 10228–10233.
[61] M. Mazaheri, A.A. Moosavi-Movahedi, A.A. Saboury, M.H. Rezaei, M. Shourian, M. Farhadi, N. Sheibani, Curcumin mitigates the fibrillation of Human Serum Albumin and diminishes the formation of reactive oxygen species, Protein Pept. Lett. 22 (2015) 348–353.
[62] J.P.K. Rooney, The retention time of inorganic mercury in the brain - a systematic review of the evidence, Toxicol. Appl. Pharmacol. 274 (2014) 425–435.